Physicochem. Probl. Miner. Process., 56(5), 2020, 839-848

http://www.journalssystem.com/ppmp

Physicochemical Problems of Mineral Processing

ISSN 1643-1049

Received June 28, 2020; reviewed; accepted August 03, 2020

Mineralogical study and enhanced gravity separation of gold-bearing mineral, South Eastern Desert, Egypt

Samah El-Sayed [1], N.A. Abdel-Khalek [1], E.H. El-Shatoury [2], A. Abdel-Motelib [3], M.S. Hassan [1], M.A. Abdel-Khalek [1]

[1] Central Metallurgical Research and Development Institute (CMRDI), P.O. Box 87 Helwan 11421, Cairo, Egypt

[2] Microbiology Department, Faculty of Science, Ain Shams University, Egypt

[3] Geology Department, Faculty of Science, Cairo University

Corresponding author: kalekma@yahoo.com (M.A. Abdel-Khalek)

Abstract: El-Hudi gold deposit, located in the South Eastern Desert of Egypt, represent large vein- type gold occurrence. The representative sample revealed the abundance of quartz as main constituent with minor amounts of mineral impurities. Gold was detectable (12 g/t) as determined using atomic absorption. The petrographic study revealed that the gold grains ranged from 10-40 μm. The grain boundaries of quartz are highly stained with iron minerals as hematite and limonite. Sericite mineral is common in discrete gold-bearing veins. Eroded pyrite was detected with high alteration leaving only cubic-shaped cavities behind. Different techniques for gravity separation were used to separate gold from the quartz mineral. After crushing and grinding of the sample, shaking table was used to upgrade the coarser fractions while Falcon concentrator was employed to upgrade the fine fraction. The best concentrate was obtained through grinding the whole sample to less than 0.2 mm, followed by cleaning steps. The gold content is increased from 12 to 145 g/t with total recovery of 78%.

Keywords: gold, mineralogy, petrography, gravity separation, Falcon concentrator

1. Introduction

Gold element has unique character and properties. It is characteristic of high resistance to chemical reagents. Gold has wider applications rather than jewelry such such as its special application in electronic circuits. It is usually found in trace amounts everywhere around the world. The largest deposits are rarely occurring (Duckenfield, 2016). The gold bearing rocks are classified into more than twenty types according to its composition. It can be occurred as metallic form or as compounds such as sulfides. Gold occurs in hydrothermal veins deposited by ascending solutions, as disseminated particles through some sulfide deposits, and in placer deposits (Zoheir, 2012).

Generally, the gold content decreases with depth (Al-Hwaiti et al, 2010), whereas the gold was exploited mainly from quartz-veins down to a depth of about 160 m. The quartz-veins and vienlets of some ores are the main sources of exploited gold (Abd El Rahim et al., 2013; Harraz, 2000; El Shemi, 2005). There are two main episodes of terrane amalgamation in the South East Egyptian Desert (Abdeen and Abdel-Ghaffar, 2011). More than 95 localities of ancient gold mines in the Eastern Desert of Egypt have been reported (Abdel-Rahim et al., 2013; Abdel-Salam et al., 2003). The gold-mineralized, quartz-veins are hosted in the granitic rocks and had been extensively exploited since the Pharaonic times until1958 (Raslan and Ali, 2010). The quartz-calcite veins contain about 30 g/t of gold; while the silver content is about 23 g/t (Abdel-Rahim et al., 2013). The shear zones and wrench faults dominate the gold distribution in the Eastern Desert of Egypt (Helmy et al., 2004; Zoheir, 2011). Gold deposits over the South Eastern Desert are generally regarded to striking shear of northwest zone. It is reflecting reactivated accretion suture zones (Zoheir, 2008). However, auriferous quartz veins confined to NNE-striking zones along the Allaqi Heiani Gerf Onib Sol Hamed Yanbu suture are only present in the Hudi

DOI: 10.37190/ppmp/125977

deposits. Scarcity of information on this deposit is attributed to its remoteness and relative inaccessibility (Rhodes and Penna, 2009).

International statistics indicate that South Africa was the world's largest gold producer for decades until 2006. Its gold output has been declining in recent years. Many other countries, in contrast, have been ramping up their production. However, no country has been able to match South Africa's peak production of above 1,000 tons per year in the 1970s. Table 1 shows the top 10 gold producing countries in the world according to the report of GFMS Gold Survey (U.S. Geological Survey, 2019). The report blamed environmental concerns, rising costs, and the crackdown on illegal mining operations for the lower output.

Table 1. World production of gold (U.S. Geological Survey, 2019)

Country	Metric Tons
China	440
Australia	300
Russia	255
United States	245
Canada	180
Peru	155
South Africa	145
Mexico	110
Uzbekistan	100
Brazil	85
Egypt	15

Pure gold has a specific gravity of 19.3 g/cm^3. Specific gravity decreases as gold naturally alloys with silver, copper or other metals. Because of the large difference between gold specific gravity and its associated minerals, most notably silica, it is separated by gravity separation processes.

Usually, gold is concentrated in its ores using the gravity, flotation or cyanidation techniques. The gravity technique is cost effective and environmentally friendly. A concentrate of 620 g/t gold with 41% recovery is produced from the Turkish gold ore, which contains 6 g/t gold, using the Knelson concentrator (Gul et al., 2012). Another concentrate of 469 g/t gold with 48% recovery is produced from the -53 micron fraction contains 8 g/t gold, using the Falcon concentrator (Onel and Tanriverdi, 2016). The shaking table has been applied for upgrading of the Central Java gold ore. The optimum gold grade is obtained from the size fraction of 87 microns. The gold particle in the finer size fraction has flaked shape which decreases its specific gravity (Ernawati et al., 2019). The processing of Zambia gold deposit produced a grade and recovery of 91 g/t and 57%, respectively, from the original ore of 16 g/t using the shaking table (Wang et al., 2019).

This work aims to evaluate representative samples from El-Hudi area and upgrading it using conventional and enhanced gravity separation.

2. Materials and methods

A representative rock sample was collected from El-Hudi gold deposit in the south eastern desert, Egypt. All chemicals used were of analytical grade from Sigma-Aldrich.

2.1. Sample preparation

The representative sample, weighing about 60 kg, was primarily subjected to crushing using a pilot unit of 5×6 inch "Denver" jaw crusher to 100% below 10 mm. The Yard sampling of the thoroughly mixed ore was done by the cone and a quartering method to get a representative 5 kg sample for granulometric analysis. The primarily crushed sample was further secondary jaw crushed to 100% below 3 mm. For preparation of the feed for gravity separation, the crushed product was finely ground to different sizes via rod milling using "Wedag" rod mill. The rod milling conditions were 6 stainless steel rods (22.8 cm length × 1.9 cm diameter) for 20 min at 1:1 solid to water. A laboratory "Wedag" Ro-tap sieve shaker

was employed for dry screening of the ore using German "Din" set sieves 8, 6.6, 4, 3.2, 2.3, 1.1, 0.8, 0.5, 0.3, 0.2, 0.125, 0.106, 0.075 mm. The time of screening was fixed at 20 min.

2.2. Sample characterization

2.2.1. X-ray diffraction (XRD)

Phase analysis of the sample was carried out "Philips type 1710 XRD unit" with Ni filter Cu radiation (Kα = 1.5446 Å) at 40 kV and 20 mA at scanning speed of one theta degree per min.

2.2.2. Chemical analysis

Complete chemical analysis of the sample was determined using "Rigakusuper Mini 200" X-ray fluorescence. The sample was pressed into a pellet through mixing 10 g of the sample with 3 g of Boreox BM-0008 binder and the mixture were subjected to 20 ton press using "Fluxana PR-25N" for 20 Sec.

Trace amount of gold was determined through wet analysis using atomic absorption technique, Perkin Elmer, Model AAnalyst-200, after digestion of 5 g of the sample with hydrochloric and nitric acids (1:3) (Ramesh et al, 2001).

2.2.3. Petrographic study

Thin and polished sections were prepared from handpicked species of the rock sample for the investigation. The petrographic study was achieved using Zeiss polarizing microscope attached to the computer program analyzer (Olympus analysis digital image solution). Polished thin-sections were studied under reflected and transmitted light respectively in order to determine mineral associations and parageneses.

2.3. Gravity concentration

Pilot scale shaking table was employed for upgrading of coarse size fractions (-0.8+0.2 and -2 +0.075 mm). Falcon concentrator as enhanced gravity separator, Sepro mineral systems, Model SB-40 semi-continuous centrifuge, the unit was used for recovery of gold from fine size fraction (-0.075 mm). The fine fraction (-0.075 mm) of the ground sample was used as a feed for Falcon Concentrator. The ground gold sample was introduced as slurry of 20 % solids through the central vertical feed pipe with feed flow rate of 0.5 L/min and accelerated by a high speed impeller at a frequency of 60 Hz (equivalent to 176 times as gravitational force). The separation was carried out at water fluidized bed pressure of 6 Psi.

3. Results and discussion

3.1. Evaluation of gold bearing rock

XRD analysis showed that the quartz is the main constituent. The other minor constituents couldn't be detected (Fig. 1). XRF analysis confirmed that it is mainly composed of SiO_2 (96.5%) with little amounts of oxides such as Fe_2O_3, Al_2O_3, CaO, Na_2O, etc., Table 2.

A 12 g/t of gold was estimated using Atomic absorption. The gold content is almost equally distributed in different size fractions except in the fine fraction size (less than 0.106 mm). The coarse size fractions (more than 4 mm) represent 61% of the sample weight, which contains about 62% of the gold content. Table 3, represent the particle size distribution for the crushed original gold bearing mineral sample.

The petrographic study using a polarizing microscope showed that the gold grains ranged in size from 10 – 40 μm. All quartz grains are thoroughly micro-fractured, as illustrated in Fig.2. It seems that the concentration of fluid inclusions (fluid inclusions are small portions of fluid, which are trapped in a solid crystal as it grew or recrystallize) increases in the micro-fractures. The grain boundaries of quartz are either very straight or bulging highly stained with iron oxide and oxy-hydroxide (Quartz grains are rimmed by fine-grained hematite and Limonite), Fig.2. These iron oxides and hydroxides are later-stage minerals. Also, hematite and limonite minerals are found as scales.

Sericite mineral is common in discrete gold-bearing veins. It is very fine, ragged grains and aggregates of white (colorless) micas, typically made of muscovite which is a hydrated phyllo-silicate mineral [$KAl_2(AlSi_3O_{10})(FOH)_2$], illite or paragonite [$NaAl_2[(OH)_2AlSi_3O_{10}]$. Sericite is produced by alteration of orthoclase ($KAlSi_3O_8$) or plagioclase feldspars ($KAlSi_3O_8$–$NaAlSi_3O_8$–$CaAl_2Si_2O_8$), Fig.3 (Guarino et al., 2011; Meunie and Velde, 2013; Anderson and Anderson, 2010; Nesse, 2012).

It contains also eroded pyrite but a large portion of pyrite has been altered or weathered leaving only cubic-shaped cavities behind. Suhedral, grained quartz can be found in these cavities. The hand sample has a druse-like texture. Reddish orange hematite and limonite occur due to complete alteration of pyrite. The grains of quartz are appearing as cloudy due to the fluid inclusions in them, Fig.4.

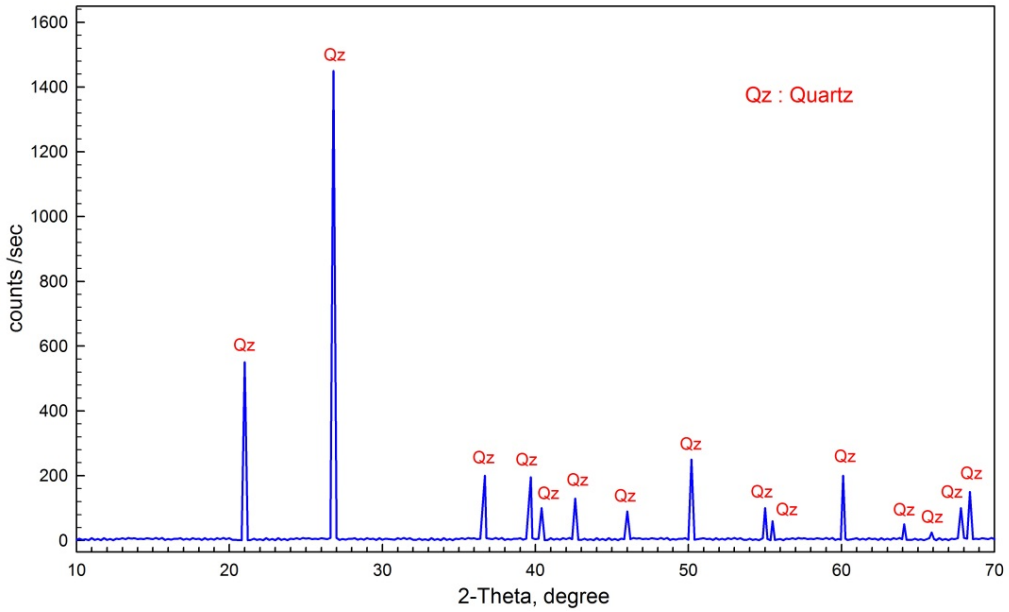

Fig. 1. XRD pattern of gold bearing mineral ore sample

Table 2. Chemical analysis by X-ray fluorescence of the run of mine sample

Item	SiO_2	Al_2O_3	Fe_2O_3	CaO	MgO	Na_2O	K_2O	SO_3	P_2O_5	Cr_2O_3	TiO_2	Co_3O_4
%	96.5	0.667	1.854	0.18	0.08	0.17	0.09	0.12	0.04	0.05	0.05	0.065

Table 3. Size analysis and gold distribution of the crushed ore sample

Size, mm	Wt%	Cumulative Wt% Retained	Gold, g/t	Gold Distribution, %
-10 +8.00	23.2	23.2	11.6	22.00
-8.00 +6.68	14.2	37.4	12.4	14.39
-6.68 +4.00	24.1	61.5	12.7	25.03
-4.00 +3.20	6.0	67.5	11.9	5.84
-3.20 +2.36	7.9	75.4	12.1	7.82
-2.36 +1.16	10.9	86.3	12.8	11.41
-1.16 +0.85	3.8	90.1	12.4	3.85
-0.85 +0.50	3.6	93.7	13.1	3.86
-0.50 +0.30	2.0	95.7	13.7	2.24
-0.30 +0.208	0.9	96.6	13.9	1.02
-0.208 +0.125	1.3	97.9	12.2	1.29
-0.125 +0.106	0.3	98.2	11.8	0.29
-0.106 +0.075	0.9	99.1	8.4	0.62
-0.075	0.9	100	4.6	0.34
Total	100.0		12.23	100.0
Head	100.0		12.07	100.0

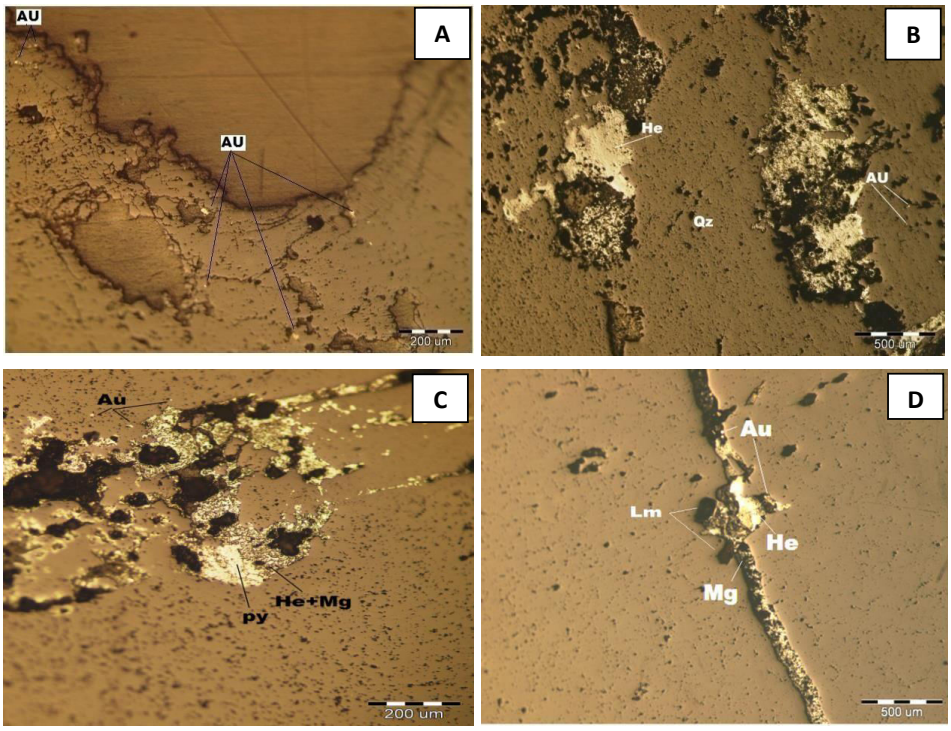

Fig. 2. Photomicrograph shows gold grains, 10-40 µm (A & B) and grain boundaries of quartz (very straight or bulging highly stained with hematite (C) and limonite (D)

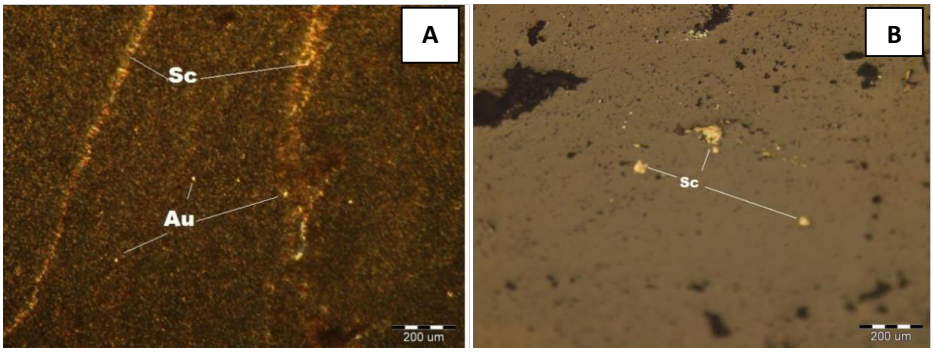

Fig. 3. Photomicrograph shows sericite mineral is common in discrete gold-bearing veins ragged grains (A) and aggregates of white micas, illite or paragonite (B)

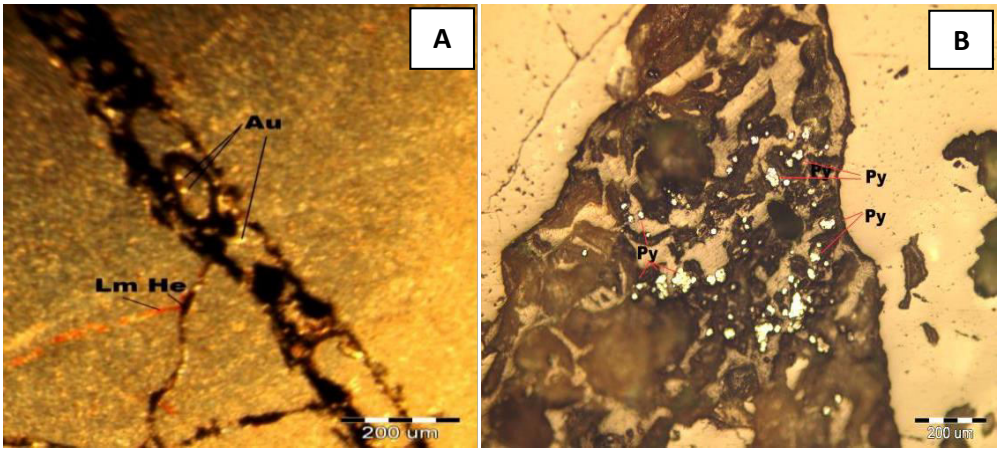

Fig. 4. Photomicrograph shows hematite and limonite occur due to complete alteration of pyrite (A) and also, eroded pyrite weathered leaving cubic-shaped cavities occupied by suhedral (B)

Pyrite is another main vein mineral occurs as fine- to medium-grained (5–30 μm). Intense alteration and weathering of pyrite can be observed in the thin section. The degree of limonite alteration in pyrite varies: pyrite grains have been replaced by limonite only partly from the edges or replaced completely, resulting in cubic limonite pseudomorphs, Fig.5. The pyrite is seen as anhedral grains and is classified as post-deformation mineralization. The tourmaline mineral group is chemically one of the most complicated groups of silicate minerals, Fig.5. It has a different composition due to replacement of isomorphous (solid solution). The general compositions can be expressed as $[XY_3Z_6(T_6O_{18})(BO_3)_3V_3W]$, where - **X** ($Ca^{2+}$, Na^{+}, K^{+}); **Y** (Li^{+}, Mg^{2+}, Fe^{2+}, Mn^{2+}, Zn^{2+}, Al^{3+}, Cr^{3+}, V^{3+}, Fe^{3+}, Ti^{4+}); **Z** (Mg^{2+}, Al^{3+}, Fe^{3+}, Cr^{3+}, V^{3+}); **T** (Si^{4+}, Al^{3+}); **V** (OH^{-}, O^{2-}); **W** (OH^{-}, F^{-}, O^{2-}).

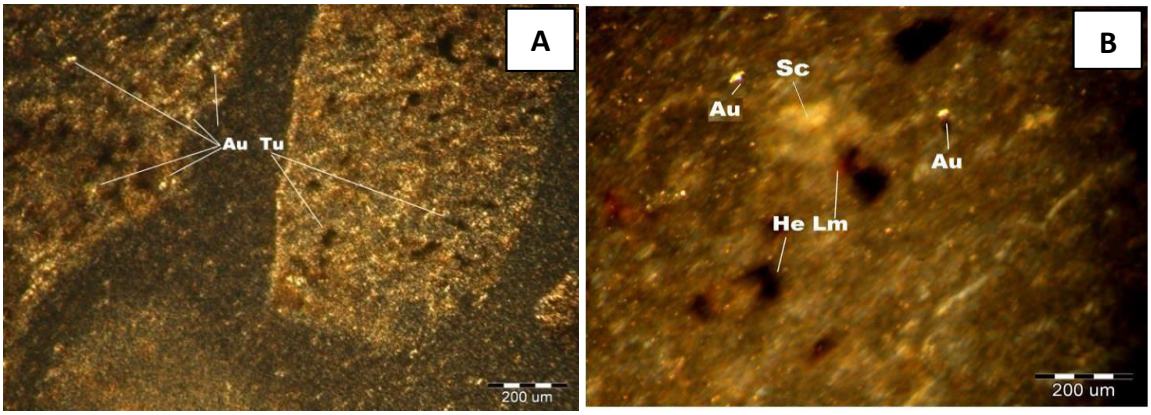

Fig. 5. Photomicrograph shows pyrite as a main vein mineral, 5–30 μm (A) and its replacement by limonite and tourmaline mineral group which is the most complicated silicate minerals (B)

3.2. Upgrading of gold sample using gravity separation

Gravity concentration techniques depends on the high difference in specific gravity between gold and its associating gangue minerals. The gold metal has a specific gravity of 19.3, and typical ore has a specific gravity of about 2.6. All gravity concentration devices create movement between the gold and host rock particles in a manner to separate the heavy pieces from the lighter pieces of material (Willsetal., 2016).

Common gravity separation equipment includes shaking table, spiral chute, and jigging concentrator. The effectiveness of gravity separation equipment is closely related to the size and shape characterizations of gold particles (McGrath et al., 2015; Jena et al., 2017). In this study, three different feeds were prepared by grinding the whole sample to less than 0.8 mm, less than 0.2 mm and less than 0.075 mm. The size analysis and gold content of each fraction is illustrated in Table 4.

Shaking table was employed for conventional gravity separation for coarse fraction (-0.8 +0.2 mm and (-0.2 +0.075 mm), while the fine fraction (-0.075 mm) was subjected for upgrading using falcon concentrator. Shaking tables are effective in the processing of material in the size range 3 mm to 15 μm according to Ernawati et al., (2019). Table 5 shows the recovery and gold assay of the products resulting from processing of ground sample of less than 0.8 mm. It is clear that the processing of coarse fractions (-0.8 +0.2 mm and -0.2 +0.075 mm) did not give good results in comparison to fine fraction (-0.075 mm). Adams (2016) recorded that up to 90% of coarser gold than 40 μm can be recovered, whereas typically only 20% of 20-40 μm gold can be recovered and the efficiency drops greatly below 40 μm. Falcon concentrator can achieve up to 99% recovery efficiency below 30 μm (Ernawati et al., 2019).

Table 6 shows the recovery and gold assay of the products resulting from processing of ground sample of less than 0.2 mm. It is clear that the processing of fine fraction (–0.075 mm) led to better results compared to that of the coarser fraction (–0.2 +0.075 mm).

Table 7 shows the recovery and gold assay of the products resulting from processing of ground sample of 100% less than 0.075 mm. Although the concentrate has a higher recovery (95%) compared to Onel and Tanriverdi (2016) who achieved recovery, 72% with the same size, the gold content is lower than that obtained from the processing of the sample ground 100% below –0.2 mm.

Table 4. Grinding the whole sample to three different sizes

Ground product	Size, mm	Wt%	Gold (g/t)
Feed (1): 100% less than 0.8 mm	-0.8 +0.2	42.58	13.28
	-0.2+0.075	26.61	12.76
	-0.075	27.81	2.43
	Total	100	12.07
Feed (2): 100% less than 0.2mm	-0.2+0.075	38.70	15.80
	-0.075	61.30	11.84
	Total	100	12.07
Feed (3): 100% less than 0.075 mm	-0.075	100	12.12
	Total	100	12.07

Table 5. Recovery and assay results of gravity separation for ground sample (–0.8 mm)

Top size	Fraction	Process	Product	Gold (g/t)	Rec.%	Total Rec.%
Feed (1): 100 % less than 0.8 mm	–0.8 +0.2	Shaking Table	Concentrate 1	15.27	6.79	3.80
			Tailing 1	13.15	93.21	52.14
			Head	13.28	100.00	55.93
	–0.2 +0.075	Shaking Table	Concentrate 2	24.12	15.51	5.79
			Tailing 2	11.74	84.49	31.58
			Head	12.76	100.00	37.37
	–0.075	Falcon	Concentrate 3	68.51	76.01	5.09
			Tailing 3	0.60	23.99	1.61
			Head	2.43	100.00	6.70
Result Summary		Concentrate 1,2,3		26.07		14.68
		Tailing 1,2,3		9.14		85.32
		Head		10.11		100.0

Table 6. Recovery and assay results of gravity separation for ground sample (–0.2 mm)

Top size	Fraction	Process	Product	Gold (g/t)	Rec.%	Total Rec.%
Feed (2): 100 % less than 0.2 mm	–0.2 +0.075	Shaking Table	Concentrate 4	67.74	62.60	28.62
			Tailing 4	6.92	37.40	17.10
			Head	15.80	100.00	45.73
	–0.075	Falcon	Concentrate 5	147.47	92.18	50.03
			Tailing 5	1.00	7.82	4.25
			Head	11.84	100.00	54.27
Result summary		Concentrate 4,5		103.25		78.65
		Tailing 4,5		3.18		21.35
		Head		13.37		100.00

Table 7. Recovery and assay results of gravity separation for ground sample (–0.075 mm)

Top size	Fraction	Process	Product	Gold (g/t)	Rec.%	Total Rec.%
Feed (3): 100 % –0.075 mm	–0.075	Falcon	Concentrate 6	52.45	95.17	95.17
			Tailing 6	0.75	4.83	4.83
			Head	12.12	100.00	100.00
Result summary		Concentrate 6		52.45		95.17
		Head		12.12		95.17

The above results were summarized in Table 8. It showed that the gold is increased from 12 to 26 g/t with total recovery of 14.7% through the upgrading of the ground whole sample to less than 0.8 mm. The gold increased from 12 to 103 g/t with total recovery of 78.6% through the upgrading of the ground whole sample to less than 0.2 mm. On the other hand, although the total recovery was 95.17%in the sample ground 100% below 0.075 mm, the gold increased from 12 to 52 g/t only. Falcon concentrator was used to treat the tailings of Nicaraguan gold ore with particle sizes below 20 µm and achieve 59.4 wt% recovery (Gul et al., 2012).

Table 8. Summary of gravity separation results for three ground samples

Top Size	Product	Gold (g/t)	Total Rec.%
(100% –0.8 mm)	Concentrate 1,2,3	26.07	14.68
(100% –0.2 mm)	Concentrate 4,5	103.25	78.65
(100% –0.075 mm)	Concentrate 6	52.45	95.17
Head		12.07	100

3.3. Cleaning of rougher products

To improve the gold grade, the products of upgrading samples were ground to less than 0.075 mm, followed by further concentration using Falcon concentrator. According to Ernawati et al., (2019) recovery is effective down to approximately 30 µm using falcon concentrator. The results were illustrated in Tables 9 and 10.

Table 9. Results of gravity separation after cleaning for ground sample (–0.8 mm)

Top size	Fraction	Process	Product	Gold (g/t)	Rec.%	Total Rec.%
Feed (1): 100 % less than 0.8 mm	Tail 1 –0.8 +0.2	Falcon	Concentrate 7	59.77	8.88	4.63
			Tailing 7	8.61	91.12	47.51
			Head	13.15	100.0	52.14
	Tail 2 –0.2+0.075	Falcon	Concentrate 8	69.81	6.79	8.82
			Tailing 8	9.01	93.21	23.07
			Head	11.86	100.0	31.89
	–0.8 +0.2	Falcon	Concentrate 1	15.27	6.79	3.80
	–0.2 +0.075		Concentrate 2	24.12	15.51	5.79
	–0.075		Concentrate 3	68.51	76.01	5.09
Summary		Concentrate 1,2,3,7,8		39.87		28.13
		Head		10.11		100.0

Table 10. Results of gravity separation after cleaning for ground sample (–0.2 mm)

Top size	Fraction	Process	Product	Gold (g/t)	Rec.%	Total Rec.%
Feed (2): 100 % less than 0.2 mm	Tail 4 –0.2 +0.075	Falcon	Concentrate 9	30.69	6.79	1.16
			Tailing 9	6.00	93.21	15.94
			Head	6.99	100.0	17.10
	Conc. 4 –0.2 +0.075	Falcon	Concentrate 10	142.04	94.92	27.17
			Tailing 10	6.27	5.08	1.45
			Head	67.74	100.0	28.62
	–0.075	Falcon	Concentrate 5	147.47	92.18	50.03
			Tailing 5	1.00	7.82	4.25
			Head	11.84	100.0	54.27
Summary		Concentrate 5,9,10		145.52		78.36
		Head		13.37		100.0

The results were summarized in Table 11. These results showed that the gold concentration increased from 12 to 37.9 g/t with total recovery of 28% through grindingthe whole sample to less than 0.8 mm. For grinding the sample to 100% less than 0.2 mm, the gold is increased from 12 to 145.5 g/t with total recovery of 78.36 %. Although the resulting concentrate is not sufficiently high in grade compared to previous research, this is reflected in a high recovery (Gul et al., 2012; Onel and Tanriverdi, 2016; Ernawati et al., 2019; Wang et al., 2019).

Table 11. Summary of gravity separation results for three ground samples with a cleaning stage.

Top Size	Product	Gold (g/t)	Total Rec.%
(100% –0.8 mm)	Concentrate 1,2,3,7,8	39.87	28.13
(100% –0.2 mm)	Concentrate 5,9,10	145.52	78.36
(100% –0.075 mm)	Concentrate 6	52.45	95.17
Head		12.07	100

4. Conclusions

El-Hudi gold deposit, located in the South Eastern Desert of Egypt, represent large vein- type gold occurrence. X-ray fluorescence analysis of the mine sample showed the abundance of SiO_2 (96.5%) with traces of Fe_2O_3, Al_2O_3, CaO, Na_2O, etc. The sample contains trace amount of gold (12 g/t).

Microscopic study of thin and polished sections showed that the gold grains ranged in size from 10 – 40 μm. All quartz grains are thoroughly micro-fractured. The grain boundaries of quartz are straight or bulging highly stained with iron oxide and oxy-hydroxide. Also, scales of hematite and limonite are noted. Sericite mineral is common in discrete gold-bearing veins. It contains also eroded pyrite but a large portion of pyrite has been altered or weathered leaving only cubic-shaped cavities behind. The tourmaline mineral group is chemically one of the most complicated groups of silicate minerals.

Three different feeds were prepared by grinding the whole sample to 100% less than 0.8, 0.2 and 0.075 mm. Shaking table was employed as a conventional gravity separation technique for coarse fraction (-0.8 +0.2 mm and -0.2 +0.075 mm), while the fine fractions (-0.075 mm) were upgraded using the Falcon concentrator unit.

A concentrate of 26 g/t with total recovery of 14.7% was obtained from sample ground 100%to less than 0.8 mm. Cleaning steps, increased the gold to 37.9 g/t with total recovery 28%. A second concentrate contains 103 g/t with total recovery of 78.6% was obtained through grinding the sample to 100% less than 0.2 mm. Cleaning steps, increased the gold to 145 g/t with the same recovery (78%). A Third concentrate of 52 g/t only with total recovery of 95.1% was obtained through grinding whole sample to 100% less than 0.075 mm. Although the third concentrate has the maximum recovery (95.17%), the second concentrate is considered the best, in terms of its assay (about 145 g/t) and good recovery (78%).

References

ABDEEN, M.M., ABDEL-GHAFFAR, A.A., 2011. *Syn- and post-accretionary structures in the Neoproterozoic central Allaqi-Heiani suture zone, southeastern Egypt*. Precambrian Research 185, 95-108.

ABDEL-RAHIM, S.H., EL-NASHAR, E.R., OSMAN, A.F., ABDEL-GHAFFAR, N.I., 2013. *Gold-Bearing sulfides associated with granitic wall-rock alterations at Fawakhir Area, Central Eastern Desert*, Egypt, Journal of Applied Sciences Research, 9(11): 5878-5903.

ABDEL-SALAM, M.G., ABDEEN, M.M., DOWIDAR, H.M., STERN, R.J., ABDEL-GHAFFAR, A.A., 2003. *Structural evolution of Neoproterozoic Western Allaqie Heiani suture, South Eastern Egypt*. Precambrian Research 124, 87-104.

ADAMS, M., 2016. *Gold Ore Processing: Project Development and Operations (2nd ed)*. Fugue Pet Ltd, Singapore.

AL-HWAITI, M., ZOHEIR, B., LEHMANN, B., RABB, I., 2010. *Epithermal gold mineralization at Wadi Abu Khushayba, southwestern Jordan*. Ore Geology Reviews, 38, 1–2, 101-112.

ANDERSON, R.S., ANDERSON, S.P., 2010. *Geomorphology: The Mechanics and Chemistry of Landscapes*, Cambridge University Press., 187.

DUCKENFIEL, M., 2016. *Monetary History of Gold: A Documentary History, 1660-1999 1st ed*. Kindle Edition, ISBN-13: 978-1851967858, Amazon Digital Services LLC.

EL-SHAMI, A.M., 2005. *Structural control of the gold bearing quartz veins*, Sci. Bull., Minia Univ., 16(2): 45-62.

ERNAWATI, R., IDRUS, A., PETRUS, H.T.B.M., 2019. *Study of the optimization of gold ore concentration using gravity separator (shaking table): case study for LS epithermal gold deposit in Artisanal Small scale Gold Mining (ASGM) Paningkaban, Banyumas*, Central Java IOP Conf. Ser.: Earth Environ. Sci. 212 012019

GUARINO, V., FEDEL, L., FRANCIOSI, L., LONIS, R., LUSTRINO, M, MARRAZZO, M., MELLUSO, L., MORRA, V., ROCCO, I., RONGA, F., 2011. *Mineral compositions and magmatic evolution of the calcalkaline rocks of northwestern Sardinia, Italy*. Periodico di Mineralogia, 80, 3 (Spec. Issue), 517-545.

GUL, A., KANGAL, O., SIRKECI, A.A., ONAL, G., 2012. *Beneficiation of the gold bearing ore by gravity and flotation*. International Journal of Minerals, Metallurgy and Materials, 19, 2, 106.

HARRAZ, H.Z., 2000. *A genetic model for a mesothermal Au deposit: evidence from fluid inclusions and stable isotopic studies at El Sid Gold Mine, Eastern Desert, Egypt*. J. African Earth Sci., 30(2): 267-282.

HELMY, H.M., KAINDL, R., FRITZ, H., LOIZENBAUER, J., 2004. *The Sukari gold mine, Eastern Desert-Egypt: Structural setting, mineralogy and fluid inclusion study*. Mineralium Deposita 39, 495-511.

JENA, M.S., MOHANY, J.K., SAHU, P., VENUGOPAL, R., MANDRE, N.R., 2017. *Characterization and Pre-concentration of Low Grade PGE Ores of Boula Area, Odisha using Gravity Concentration Methods*. Trans. Indian Inst. Met., 70, 287–302.

MC-GRATH, T.D.H., CONNOR, L.O., EKSTEEN, J.J., 2015. *A comparison of 2D and 3D shape characterization of free gold particles in gravity and flash flotation concentrates*. Miner. Eng., 82, 45–53.

MEUNIER, A., VELDE, B., 2013. *Illite: Origins, Evolution and Metamorphism, Springer, ISBN 978-3-662-07850-1.*

NESSE, W.D., 2012. Introduction to mineralogy (2nd ed.) New York: Oxford University Press. ISBN:978-0199827381.

ONEL, O., TANRIVERDI, M., 2016. *Use of Falcon Concentrator to Determine the Gravity Recoverable Gold (GRG) Content in Gold Ores*. Journal of the Polish Mineral Engineering Society, 17(1): 189-194.

RAMESH, S.L., SUNDER, RAJU, P.V., ANJAIAH, RAMAVATHI MATHUR K.V., GNANESWARA, RAO T., DASARAM, B., NIRMAL, CHARAN S., SUBBA, RAO D.V., SARMA, D.S., RAM, MOHAN M., BALARAM, V., 2001. *Determination of Gold by Atomic Absorption Techniques*. PerkinElmer Instruments LLC, 22(1).

RASLAN, M.F., ALI, M.A., 2010. *Mineral chemistry of polymetallic mineralization associated with altered granite, Hangaliya area, South Eastern Desert, Egypt*. GEOLOGIJA 53/2, 129-138, Ljubljana.

RHODES, M., PENNA, F., 2009. *Flowsheet development for the Sukari gold project in Egypt*, World Gold Conference 2009, The Southern African Institute of Mining and Metallurgy.

U.S. Geological Survey, *Mineral Commodity Summaries*, 2019. https:prd-wret.s3-us-west-2. Amazonaws.com/ assets/palladium/production/atoms/files/mcs2019-all.pdf.

WANG, X., QIN, W., JIAO, F., YANG, CUI, Y., LI, W., ZHANG, Z., SONG, H., 2019. *Mineralogy & Pretreatment of a Refractory Gold Deposit in Zambia*, Minerals, 9, 406.

WILLS, B.A., FINCH, J.A., 2016. FRSC, FCIM, P. Eng., in Wills' Mineral Processing Technology (18th ed).

ZOHEIR, B.A., 2008. *Characteristics and genesis of shear zone-related gold mineralization in Egypt: a case study from the Um El Tuyor mine, South Eastern Desert*. Ore Geology Reviews 34, 445-470.

ZOHEIR, B.A., 2011. *Transpressional zones in ophiolitic mélange terranes: potential exploration targets for gold in the South Eastern Desert, Egypt*. Journal of Geochemical Exploration 111, 23-38.

ZOHEIR, B.A., 2012. *Controls on lode gold mineralization, Romite deposit, South Eastern Desert, Egypt*. Geoscience Frontiers 3(5) 571-585.